

Peter Michael Bandelt Riess
Michael Kuhn
Petra Först
Heiko Briesen*


Investigating the Effect of Packed Structures on Filter Cake Compressibility

Packed beds used in absorption columns have shown to increase filter cake permeability during specific filtration processes. Their effect on filter cake compressibility is evaluated. Different model systems are characterized using dead-end filtration equipment and a modified universal testing machine. Compression experiments are conducted with different packings to assess the systems' response to compressive stress. The structural support of the packings reduces filter cake compressibility for the tested configurations. The extent of this effect depends on packing type, applied pressure, and material compressibility. These results help to understand the advantages of using packed beds as aids for filtration processes and represent a step further in designing tailored packings.

Keywords: Cake filtration, Compressibility, Packed beds, Process strategy

Received: October 02, 2020; *revised:* January 21, 2021; *accepted:* January 25, 2021

DOI: 10.1002/ceat.202000451

 This is an open access article under the terms of the Creative Commons Attribution-NonCommercial License, which permits use, distribution and reproduction in any medium, provided the original work is properly cited and is not used for commercial purposes.



Supporting Information
available online

1 Introduction

Laboratory-scale cake filtration studies gather relevant data, which are then used in the design of industrial rotary filters, filter presses, or centrifuges, among others, for countless applications [1]. Several variables and correlations should be considered. For example, treated suspensions are very rarely ideal (monodisperse, incompressible spheres). Filter cake porosity is reduced in the direction of the filter medium in real, compressible systems, where the weight of all solid layers is supported and hydrodynamics are most affected [2]. Suspensions can show slightly to extremely high degrees of compressibility. Some examples of highly compressible substances are microcrystalline cellulose [3], wastewater sludge [4], alginate beads [5], and chromatography gels [6]. Such systems tend to form a nearly impenetrable skin at the filter medium, thus stopping the process [2]. Hence, filter cake compression is one of the fundamental phenomena and, therefore, an intensively studied subject in solid-liquid separation research.

Comparisons between two frameworks describing the dewatering of compressible suspensions have been made in recent investigations [7]. They are known as conventional filtration theory, attributed to Ruth, Tiller, and Shirato [8], and compressional rheology, developed by Buscall, White, and Landman [9]. While the former mostly uses space-averaging approaches to quantify separation descriptors empirically, the latter yields local information from a phenomenological point of view. Nevertheless, the two theories have been proven to be interchangeable and able to complement each other [7]. Hence, this study benefits from both frameworks to evaluate process strategies based on dealing with filter cake compressibility.

Several investigators, such as Alles [10], have analyzed filter cake compression in detail and derived general guidelines to handle the type of suspension accordingly. To date, numerous

strategies have been published to improve various processes one way or another. The spectrum of complexity has become very broad since the method must always be tailored to the application at hand. For example, the flow rate can be increased by using continuous [11] or discrete [12] mechanical vibrations during cake filtration. If the suspension contains paramagnetic solids, or if said solids are purposefully added to it, a magnetic field can also render more permeable filter cakes [13]. In the case of dewatering, the superposition of shear forces to increase efficiency is an ongoing subject of investigation [14]. The classic method of coagulation of water contaminants can be combined with ozone oxidation to reduce membrane fouling [15]. Antifouling behavior has also been achieved by changing the properties of the membrane, either chemically through functional groups [16] or physically through printed textures [17].

The latter makes use of a wavy structure at the filter medium to provide increased support, which alters the local hydrodynamics. Similar results were obtained for thin-film microfiltration of algae by incorporating rigid particles into the suspension [18] to reduce compression and increase porosity and flux. Coincidentally, it is known in the field of thermal separation processes that beds packed inside absorption columns can exhibit analogous channeling and preferential flow caused by wall effects [19]. Considering this, it is plausible that packed beds can be purposefully applied to filtration processes as an

Peter Michael Bandelt Riess, Dr.-Ing. Michael Kuhn, Prof. Dr.-Ing. Petra Först, Prof. Dr.-Ing. Heiko Briesen
briesen@wzw.tum.de

Technical University of Munich, TUM School of Life Sciences Weihenstephan, Chair of Process Systems Engineering, Gregor-Mendel-Strasse 4, 85354 Freising, Germany.

alternative method for incorporating wall support and counter-acting compression.

This strategy was already put to the test by Bandelt Riess et al. [20]. Random and structured packings were assessed using averaging approaches within the context of cake-forming filtration for three model systems. In the case of two nearly incompressible model systems, the packings exhibited a negative effect, adding resistance to the cake and prolonging separation time. However, a very positive effect on the filtration of a highly compressible biological suspension was identified and separation time was strikingly shortened.

These observations may be related to those made in the field of high-performance liquid chromatography by Lan et al. [21] and Lan [22]. They implemented a systematic enhancement of cylindrical wall support in a chromatography column packed with compressible resins. By doing so, the same level of resin compression was achieved at a much higher critical flow velocity. They demonstrated that the results were, among others, dependent on the material properties of the resins, e.g., Young's modulus. For this reason, it would be interesting to consider this correlation when studying solid-liquid separations as well.

Bandelt Riess et al. [20] initially proposed that packings caused two types of effects when used for cake filtration: a so-called steady-state effect, which is based on filter cake permeability, and a transient-state effect, which is based on filter cake compressibility. In the first case, more porous and permeable structures could be formed when incorporating the packed beds into the filter, and therefore specific flow resistance was reduced for a fixed operating pressure. The second case considers forces that interact within the cake itself during separation. As the structure collapses under stress, additional wall support can oppose this effect through friction. However, a more detailed characterization of the systems regarding their compressibility associated with packed beds has not yet been reported.

This study aims to close the gap and investigates the effects of packings on filter cake compressibility. Finding a correlation between operating pressure, cake compression factor, and packing influence is proposed, which would clarify the aforementioned transient effects of this strategy. Once this is understood, the packing can be adapted to the particularities of a suspension of interest. To test this hypothesis, various combinations of suspended solids and packed beds are analyzed to identify the key factors that make the use of packings advantageous.

2 Materials and Methods

2.1 Model Systems

The first suspended solid is the virtually incompressible Crosspure[®] XF (CP; BASF SE). CP is a mixed extrudate made up of 70 % polystyrene and 30 % polyvinylpyrrolidone which is used in beer filtration as a filter aid. It was

selected because of its simplicity; in addition to its relative rigidity, the particles have a rather spherical shape.

The second substance, Arbocel[®] UFC 100 (AC; J. Rettenmaier & Söhne GmbH & Co. KG), is another type of filter aid made of 99.5 % cellulose fibers. The average particle size is between 6 and 12 μm . Particles can reorganize during filtration because the particle structure of AC has more degrees of freedom than CP; thus, the material should be slightly more compressible.

Hop pellets (HO; Simon H. Steiner, Hopfen, GmbH) are a good example of a complex biogenic solid. They are comprised of dried, ground hops. Once the pellets are dispersed, the system becomes noticeably polydisperse. The pellets used were of the Cascade hops variety. This variety contains 16.5 % resins, which greatly contributes to its compressibility. Fig. 1 depicts the materials.

2.2 Packed Beds

The first packing used was a random one made of Raschig rings (1400/6, Glaswarenfabrik Karl Hecht GmbH & Co. KG). Ralu rings (Raschig GmbH) were employed in a second random packing. Finally, a rather structured packing was fabricated using three standing, adjacent 25-4 Raflux rings (RVT process equipment GmbH). The packings are presented in Fig. 2, and their properties are summarized in Tab. 1.

The number of rings that were placed into the filter was determined by the number required to cover the filter area and

Table 1. Properties of the packings used in this study for one filter cake.

Type	Raschig	Ralu	Raflux
Material	Glass	Plastic	Steel
Diameter [mm]	6	15	25
Length [mm]	6	15	25
Wall thickness [mm]	1	1	0.5
Surface [m^2m^{-3}]	940	320	215
Void volume [%]	58	94	95
Ring quantity [-]	96	10	3

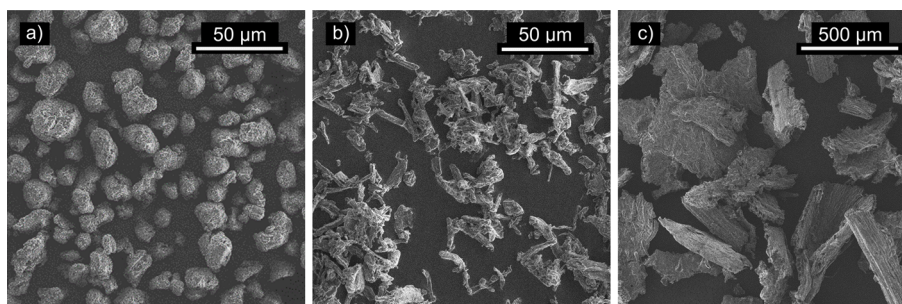


Figure 1. Scanning electron microscope images of (a) CP, (b) AC, (c) HO.

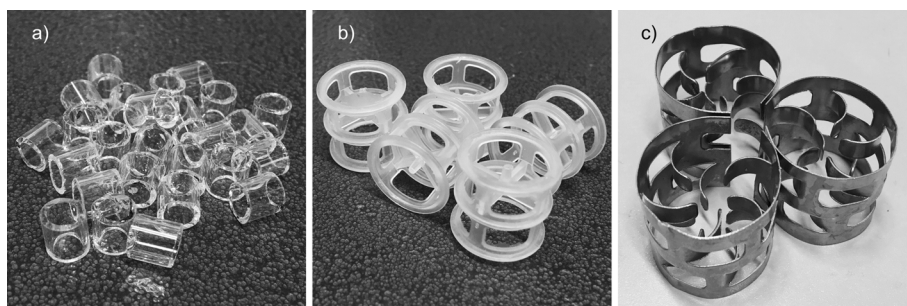


Figure 2. Photographs of (a) Raschig, (b) Ralu, (c) Raflux rings.

form a single layer of packed rings on top of the filter medium. Hence, the height of each packing was the corresponding ring length given in Tab. 1.

2.3 Particle Size Distribution Analysis

The particle size distributions (PSDs) of the model systems were analyzed in normalized differential and cumulative forms using the laser diffraction setup HELOS/KR (Sympatec GmbH) and WINDOX 5.7.0.0 software. The samples were suspended in water and uniformly dispersed in the setup using its QUIXEL dispersion unit. The lens module R2 or R7T was used depending on the particle size range.

2.4 Filtration Equipment

The filtration experiments were conducted using an experimental stand designed and built according to Association of German Engineers standards (VDI guideline 2762 Part 2). The equipment included two separate housings to disperse and then filter the suspensions under pressure. The first housing was equipped with a stirrer and had an internal diameter of 120 mm and a volume capacity of 1.7 L, whereas the second housing had an internal diameter of 100 mm, equivalent to a filtration area of 78.54 cm². DP 1575 090 filter paper (Hahnemühle FineArt GmbH) with 2 μm retention capacity was used as the filter medium. The permeate mass was measured using an automated Kern & Sohn GmbH KB 10000-1N precision scale. The data were processed using MATLAB (The MathWorks, Inc.) code. A schematic of the equipment is illustrated in Fig. 3.

2.5 Compression Equipment

The first stage of the compression experiments was conducted using a small filtration chamber, also built according to Association of German Engineers standards (VDI guideline 2762 Part 2), equipped with a detachable Plexiglas ring for filter cake accumulation. The housing had an internal diameter of 66.5 mm (filtration area of 34.68 cm²) and a volume capacity of 0.85 L. The filter medium was the above-mentioned type of filter paper. In the second stage, the same Plexiglas ring was set for piston-driven compression experiments in a universal testing machine (model zwickiLine; ZwickRoell GmbH & Co. KG).

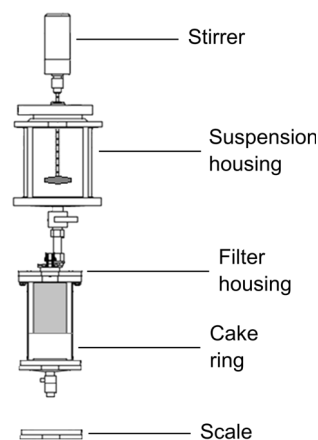


Figure 3. Experimental filtration equipment.

A base for the filter cake ring and a sealed, rigid piston with bleed line were adapted for these tests, allowing for complementary experiments and precise force and height measurements. The movement of the piston was controlled and recorded with testXpert II software (version 3.4), and the data were processed using further MATLAB (The MathWorks, Inc.) code. A schematic of the equipment is illustrated in Fig. 4. Coupling filtration with material testing represents a fast and uncomplicated method for performing this kind of experiment.

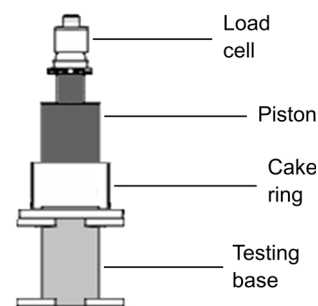


Figure 4. Experimental compression equipment.

2.6 Experimental Procedures

A series of experiments without packings was first performed for reference and characterization of the model systems and, thus, standard filtration and compression curves were obtained for each suspension and each equipment. All experiments were

performed in triplicate, and the results were expressed as the arithmetic mean value. The error bars indicate standard deviations.

Regarding the filtrations, the suspensions were separated under pressures between 0.5 and 2.0 bar to detect changes in filtrate flow caused by compression. The dead-end filtrations were conducted according to VDI guideline 2762, Part 2 [23]. Each suspension was prepared using distilled water at a final volume of 1.5 L. The CP and AC samples were weighed and presuspended in the distilled water before being homogenized in an ultrasonic tub. To disperse the HO particles, the pellets had to be submerged in water overnight before preparing the suspension. The sample quantity was determined based on a cake height of 1.1 cm for CP and AC (40 and 30 g, respectively) and 2.3 cm for HO (30 g). The latter was designed to be higher to achieve comparable filtration times for all systems.

The sample was transferred to the suspension housing after configuring its stirrer to maintain homogeneity. Subsequently, the valve leading to the filter housing was opened, the system was pressurized, and filtration and data recording were initiated.

According to the standardized norm [23], filtration data (accumulated filtrate mass over time) are to be plotted in the form of time/accumulated filtrate volume over the same volume to obtain the flow resistance of the filter medium, $R_M^{(1)}$, and relative filter cake resistance, α_K , following Eq. (1):

$$\frac{t}{V} = \frac{k\eta\alpha_K}{2A^2\Delta p} V + \frac{R_M\eta}{A\Delta p} \quad (1)$$

where t denotes the filtration time, V the filtrate volume, k a concentration constant calculated from the cake thickness, η the fluid viscosity, A the filter area, and Δp the differential pressure.

However, recent research conducted by Kuhn et al. [24] effectively showed that fitting the filtration curve nonlinearly to a root function is more precise both in terms of execution and results. Thus, the change in filtrate volume over time is described as:

$$V = \sqrt{\frac{2\Delta p A^2}{\eta\alpha_K k} t + \left(\frac{R_M A}{\alpha_K k}\right)^2} - \frac{R_M A}{\alpha_K k} \quad (2)$$

The parameters of interest were estimated by finding the deviation minimum with the usual least-squares method after choosing this fitting strategy. The procedure was repeated for every operating pressure and for each system to draw conclusions about their compressibility. This last parameter is often determined by fitting power functions, such as Eq. (3) [25, 26], to the changes in flow resistance due to increases in differential pressure.

$$\alpha_K = K_\alpha \Delta p^{N_\alpha} \quad (3)$$

Here, N_α represents global compressibility and its value can be used as a point of reference for comparison of compressible

network behavior. The coefficient K_α does not necessarily have a physical meaning but it is often associated with filter cake resistance at a low differential pressure.

For the reference filter cake compressions in the testing machine, the systems first had to be separated in the small filtration chamber under 1.0 bar, analogous to the previous method. Each suspension was prepared using distilled water at a final volume of 0.5 L. The samples were weighed, suspended, and homogenized in the ultrasonic tub as before. The quantities were again determined based on a cake height of 1.1 cm for CP and AC (15 and 10 g, respectively) and 2.3 cm for HO (10 g). The suspension was transferred directly into the filter housing, the system was closed and pressurized, and the filtrate was then purged until the wet filter cake formed in the Plexiglas ring (2 mm of liquid remained above the solid network).

Subsequently, the ring containing the filter cake was detached from the housing to be fixated and aligned below the piston of the testing machine. The starting point of the measurement was the initial filter cake height, which had been determined upon first contact with the piston. Subsequently, the piston was lowered automatically at a rate of 1 mm min^{-1} until predetermined pressures were reached, while continuously recording both force and distance to obtain characteristic compression curves for the systems. These stepped pressure tests (analogous to Usher et al. [27]) were performed seamlessly between 20 and 500 kPa, allowing the system to reach mechanical equilibrium for 20 s. The equilibrium pressure in the solid network is known as compressive yield stress p_y . The evolution of this value according to the relative variation in filter cake volume V_K was used to complement the global compressibility results of the previous method.

Furthermore, filter cake compressions were conducted with the different packings in Tab.1 to detect variations in the compression behaviors of the systems. The procedures were repeated as explained, this time after additionally placing the predetermined quantity of packed elements into the small filter chamber before transferring the suspensions. This way, the solids accumulated around and above the packings during the separation, forming layered structures. The sample quantities were previously adjusted to guarantee that the filter cake height above the packing was at least as tall as the corresponding reference filter cake. This was done to keep the piston from coming into direct contact with the packed rings during the compression experiments. The formed filter cakes were subsequently fixated and compressed in the testing machine.

Fig. 5 illustrates the example of an AC filter cake (with height (b) 1.1 cm) with Raschig rings (packing height (c) 0.6 cm). The initial combined cake height (a) of 1.7 cm was compressed to

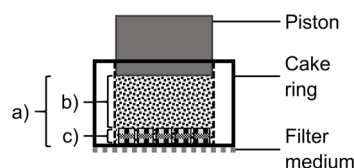


Figure 5. Schematic of a filter cake compression with packing; (a), (b), and (c) are the heights of the combined filter cake, suspended solids cake, and packing, respectively.

1) List of symbols at the end of the paper.

an end height of 1.0 cm. All compressions were performed within the extension of (b).

3 Results and Discussion

3.1 Particle Size Distribution

The results of the volumetric PSD tests are presented as characteristic values in Tab. 2. The representative variables are particle sizes $x_{10,3}$, $x_{50,3}$, and $x_{90,3}$, modal value x_h , relative span S , and specific surface S_V . The normalized differential (q_3) and accumulated forms (Q_3) of the PSDs are given in the Supporting Information.

Table 2. PSD characteristic values of the model systems.

System	CP	AC	HO
$x_{10,3}$ [μm]	10.5	2.9	58.9
$x_{50,3}$ [μm]	21.9	11.3	238.3
$x_{90,3}$ [μm]	30.3	24.9	423.4
x_h [μm]	23.0	7.2	280
S [-]	0.90	1.95	1.53
S_V [m^2cm^{-3}]	0.61	1.00	0.08

All values were estimated using laser diffraction software except for the relative PSD span S , which was determined using Eq. (4):

$$S = \frac{x_{90,3} - x_{10,3}}{x_{50,3}} \quad (4)$$

The CP sample shows a modal value that is similar to its $x_{50,3}$ value. Its PSD is rather normally distributed and relatively narrow. The AC distribution exhibits smaller characteristic values in general but a much broader relative span than that of CP. Although the AC sizes are not as evenly distributed, they are of similar orders of magnitude as the CP results and are contained within the same spectrum. HO is a more complex system where the solids consist of different substances, and it shows a distinct PSD with generally much larger values and a broad absolute span. Its S value is comparable to that of AC, also exhibiting some asymmetry in the characteristic properties of Tab. 2.

3.2 Relative Flow Resistance

During each experiment, the accumulated filtrate mass was recorded as a function of time. Furthermore, the compression behavior of the systems during filtration was assessed graphically by expressing the filtration curves according to Eq. (1) and then normalizing for differential pressure. This yields a representation for each experiment, where the gradient only depends on relative filter cake resistance. An incompressible system can be represented with a single master curve, regard-

less of the pressure [1]. An example of this method for HO is displayed in Fig. 6.

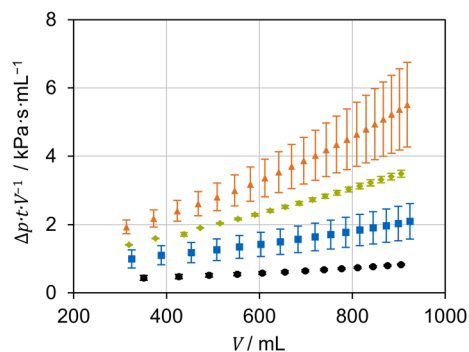


Figure 6. Pressure-normalized representation of the HO filtration curves at differential pressures of 0.5 bar (black circles), 1.0 bar (blue squares), 1.5 bar (green rhombuses), 2.0 bar (orange triangles).

The filtration runs with HO at different differential pressures are indicated and compared. It can be concluded that the system is compressed further each time, making the filter cake resistance greater since the function values grow notably when pressure is increased. This is reflected in the exponent of Eq. (3) (see Tab. 3). The same representation for all systems can be found in the Supporting Information.

Eq. (2) was employed to fit the raw filtration data to a root function by means of a least-squares method. The obtained function parameters were used to solve for the space-averaged relative flow resistance of the filter cakes. The numerical results of this study are presented in Tab. 3 for all systems.

Table 3. Relative cake resistances and global compressibilities of all systems based on filtration data.

Parameter	Δp [bar]	CP	AC	HO
α_K [10^{12}m^{-2}]	0.5	7.16 ± 1.60	6.24 ± 1.39	1.04 ± 0.11
	1.0	8.53 ± 1.16	8.08 ± 0.66	4.08 ± 0.62
	1.5	7.86 ± 1.42	9.75 ± 0.52	4.57 ± 0.45
	2.0	9.35 ± 2.85	12.36 ± 0.61	7.55 ± 1.57
N_α [-]	-	0.14 ± 0.06	0.49 ± 0.15	1.36 ± 0.02

The relative flow resistances of CP do not yield a very clear dependence on differential pressure under the given experimental conditions, as expected, since the solid is relatively incompressible. Fitting to a power function resulted in a relatively small exponent. The flow resistances of both AC and HO exhibit a considerable increase as the pressure rises, which is characteristic of plant-based suspended particles (see Fig. 1). While the former system is made up of deformable cellulose fibers, the latter resembles platelets, which can collapse under pressure. After quadrupling Δp , the flow resistance of AC doubled and that of HO increased more than sevenfold. Fitting α_K over Δp to power functions resulted in the exponents 0.49 and 1.36, respectively, making AC much more compress-

ible than CP, and, in turn, HO much more compressible than AC in this framework.

According to the VDI classification for flow resistances [23], all determined values, except AC at 2.0 bar, can be roughly considered easily separable (below $1.0 \times 10^{13} \text{ m}^{-2}$). The presented global compressibilities provide a rather qualitative overview of the compression behavior of the analyzed systems. The following results section aims at quantifying this property more accurately and introducing variations into the process.

3.3 Compression Behavior

The applied force was recorded simultaneously with the filter cake height for all compressions in the testing machine. Of the gathered data, pressures at mechanical equilibrium (compressive yield stresses) are the most relevant. For all systems and combinations, the measured values are plotted against the relative volume decrements in the network, similarly to Höfgen et al. [7].

Fig. 7 presents the different compression runs with all reference systems. A steeper slope of the curve indicates greater resistance to compressive stress. Another important property of the compression run is the abscissa of the initial value at the lowest pressure. It indicates cake height displacement between no force (at the origin) and the first compressive yield stress.

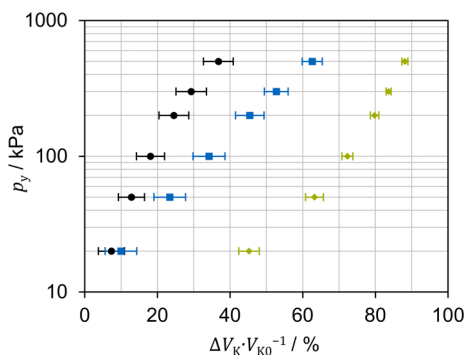


Figure 7. Compressive yield stress over relative volume change for all reference systems: CP (black circles), AC (blue squares), HO (green rhombuses).

In this regard, CP, AC, and HO exhibit respective volume reductions at the first compression of 7, 10, and 45 %. This allows for a first comparison of the systems' resistance to compressive stress, which is similar to the one in Tab. 3. With these results, however, the way networks react to a specific amount of force can be directly seen. Some differences are also observable after the first stage. The CP and AC curves start at similar values, after which the different slopes become visible. The CP slope is steeper and evidences the relative stiffness of the material again.

Since this method allows for higher pressures, it becomes possible to affect not just the particle arrangement but also the material integrity of the solids. The AC slope is smaller, spanning over a broader compression and ending at a much higher volume variation than that of CP. As expected, the HO curve exhibits the characteristic compression. It takes the lowest pres-

sure to reduce the cake height to almost half of its initial value. After this point, the curve rises similarly to CP. Compressing the already densified HO cake grows increasingly difficult since its last equilibrium is almost only 10 % of the original volume.

Thus, the differences and similarities between the materials as disperse systems and porous filter cakes have been established through standard filtration and compression experiments. The latter method is also applied to evaluate the effects of the packings used on the above-mentioned properties.

Fig. 8 shows the different compression runs with CP. For the reference (black), the filter cake is composed only of suspension solids. The colored curves correspond to the cakes including a packed bed at the bottom. Regarding the first compression step, it is not possible to identify an effect of the packings. For the tested configurations, it is necessary to overcome the pressure required to force the solid network into the packing. When the applied pressure grows, however, additional friction forces come into play and, if wall support is provided to absorb part of these forces, the resistance to stress is increased. A clear difference between the reference and all packing curves becomes visible at 300 kPa. In the end, three separate trends are identifiable, and the last reference equilibrium is at least 10 % away from the others. The Raschig and Ralu packings manage to counteract compression in a similar way, attributed to the fact that both are random and can rearrange during the experiment, and the Raflux structure has the most considerable effect.

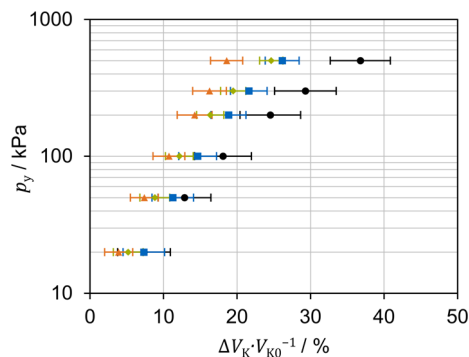


Figure 8. Compressive yield stress over relative volume change for CP: reference (black circles), Raschig rings (blue squares), Ralu rings (green rhombuses), Raflux structure (orange triangles).

In past filtration experiments [20], packings were used with CP, AC, and HO to assess changes in cake permeability. Although Fig. 7 proves that they counteracted compression in a CP cake, Ralu and Raflux rings had no influence on its permeability and the Raschig packing even reduced it. Since those effects were observed in filtrations at 1.5 bar, it is arguable that the effect of the packings was not relevant enough at such low pressures, which should be considered for future experiments. Additionally, it was discussed that the small rings exhibited a void volume lower than 60 % and therefore relatively small inner spaces, susceptible to clogging and lower permeability. Both groups of experiments lead to the conclusion that counteracting compressibility and improving permeability with packings are not necessarily coupled effects, and that further considerations must be made, such as material properties, to find a compromise.

Fig. 9 demonstrates the different runs with the more compressible AC. Regarding the compression step at 50 kPa, it is already possible to identify the influence of the packings, as opposed to CP. All three combinations noticeably decrease the volume reduction in a similar manner. As compression progresses, greater distances are put between the curves until the last reference equilibrium and its nearest one are at least 20 % away, which is a greater effect than before. The runs with Raschig and Ralu rings are practically identical up to the last point, where the latter counteracts compression more. The run with the Raflux structure represents the most stable filter cake from the start. At the end of this run, the network is even less compressed than CP. As stated before, the void space in the packing structure seems to be beneficial.

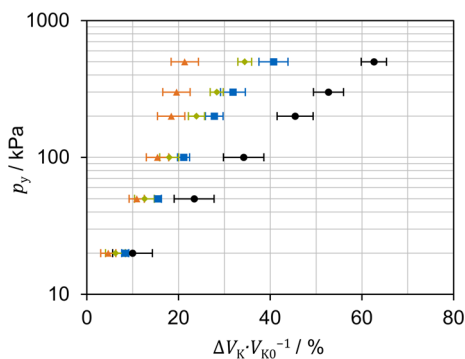


Figure 9. Compressive yield stress over relative volume change for AC: reference (black circles), Raschig rings (blue squares), Ralu rings (green rhombuses), Raflux structure (orange triangles).

Even though the packings increased resistance to compression here, they could not improve the filter cake permeability in previous investigations. It is proposed that the same forces that held the solid particles together during these experiments, opposing compressive stress and making them less compressible, are the same ones, which formed denser, less permeable cakes during the filtration experiments. Again, avoiding compression could become beneficial at higher pressures than 1.5 bar. Thus, it is possible to influence the compressibility of systems like AC favorably, while simultaneously yielding less porous networks.

Fig. 10 displays the different runs with HO. Significant differences are observed at the lowest compression step. All combinations inhibit volume reduction much better than in the previous cases, due to the compressibility of the solid network. Upon starting the experiment, the difference between the reference and its nearest curve was already approximately 6 %. As the compression progresses, greater distances appear between the reference and the Raschig and Raflux curves, respectively, while the difference to the Ralu curve remains rather constant. At the last equilibrium, four clear trends are observable in the order of the corresponding void volume. The Raflux structure stabilizes the filter cake to the point of becoming practically incompressible after the first step.

In previous filtration experiments [20], HO was the only case that exhibited permeability improvement when combined with each packing. It was proposed that the effects were caused by

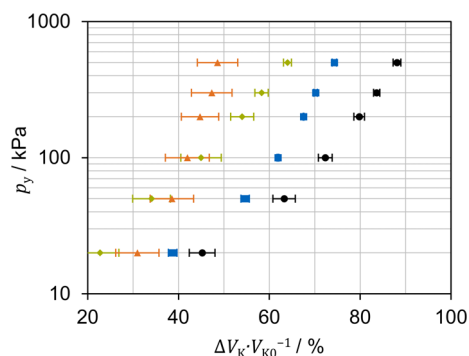


Figure 10. Compressive yield stress over relative volume change for HO: reference (black circles), Raschig rings (blue squares), Ralu rings (green rhombuses), Raflux structure (orange triangles).

the material's compressibility as well. The curves in Fig. 10 are further evidence that the greater the network compressibility, the greater the packings' effects on it. Thus, with systems like HO, it is possible to influence both the compressibility and the permeability of the solid network favorably. It is hypothesized that, due to the particle size distribution of this system and to its ratio in respect of the packing elements, forming and clogging a denser filter cake is not as plausible as with the other solids. This way, the solids form a rather porous network, which is stabilized by the packing and is compressed much less during filtration, remaining relatively porous. Hence, both compression and filtration tests were positive.

According to the results of this study, it becomes clear that filter cake compressibility has a strong influence on filtration performance, and that it can be dramatically reduced by using packings during the process. It must be stressed that the exhibited analyses are dependent on the chosen array, and it is especially challenging to quantify the influence of packings on compressibility experimentally. Therefore, different methods may complement this study in the future.

Nonetheless, the way solid particles accumulate within the filter (with or without a packed bed) has an equally considerable influence, if not more. Even if the filter cake has become less compressible, permeability can still be compromised and filtration is noticeably prolonged. A compromise between the two effects must be found for each system of interest. Thus far, the tests have been successful for HO, but testing for CP, AC, and further systems should be the aim of future investigation.

4 Conclusions and Outlook

The use of packed beds has been applied as an unconventional strategy to accelerate the separation processes of challenging biological suspensions. To evaluate the observed effects, previous studies focused on filter cake permeability and specific flow resistance without analyzing system compressibility.

Different model systems were characterized using classic filtration equipment as well as coupled filtration-compression experiments with a universal testing machine. The filter cakes were classified corresponding to their compressibility accord-

ing to both methods, showing agreement. Further compressions were conducted combining the suspended solids with defined packed configurations to analyze the effect of compressive stress on the systems. All packings provided structural support, which absorbed friction and increased compression resistance, for all systems. The greater the applied pressure or the material compressibility, the more pronounced was the effect. The fixed packing proved to be more beneficial than the random packings.

It was observed that improving compressibility is not associated with enhancing permeability. It is necessary to maintain the structure of the porous network in the process, in other words, to find a compromise. Future work should involve finding a correlation between particle size distribution and packing influence. The mentioned transient effect of this strategy may now be somewhat better understood, but the static impact is just as relevant. After that, packings can be purposefully designed for particular systems of interest.

Supporting Information

Supporting Information for this article can be found under DOI: <https://doi.org/10.1002/ceat.202000451>.

Acknowledgment

The authors would like to thank the Chair of Process Systems Engineering's workshop for their help with the hardware, and Philip Pergam for his MATLAB consultation. The practical work performed by Elena Wingerath and Maximilian Vorwerk is greatly appreciated. Open access funding enabled and organized by Projekt DEAL.

The authors have declared no conflict of interest.

Symbols used

A	$[\text{m}^2]$	filter area
K	$[\text{m}^{-2}\text{Pa}^{-N}]$	coefficient of power function
k	$[-]$	concentration constant
N	$[-]$	global compressibility
p	$[\text{bar}, \text{kPa}]$	pressure, compressive stress
Q	$[\%]$	cumulative distribution
q	$[\text{mm}^{-1}]$	normalized differential distribution
R	$[\text{m}^{-1}]$	absolute flow resistance
S	$[\text{m}^2\text{cm}^{-3}, -]$	specific surface, particle size distribution span
t	$[\text{s}]$	filtration time
V	$[\text{mL}]$	volume
x	$[\mu\text{m}]$	particle size

Greek letters

α	$[\text{m}^{-2}]$	relative flow resistance
η	$[\text{Pa s}]$	fluid viscosity

Subscripts

K	relative to filter cake
M	relative to filter medium
V	volumetric
y	vertical orientation
α	respect of relative flow resistance
0	initial condition
10	10 % accumulation
3	volumetric size distribution
50	50 % accumulation
90	90 % accumulation

Abbreviations

AC	Arbocel [®] UFC 100
CP	Crosspure [®] XF
HO	hops pellets
PSD	particle size distribution

Data Availability Statement

The data that support the findings of this study are available from the corresponding author upon reasonable request.

References

- [1] H. Anlauf, *Wet Cake Filtration: Fundamentals, Equipment, Strategies*, Wiley-VCH, Weinheim 2020.
- [2] F. M. Tiller, T. C. Green, *AIChE J.* **1973**, *19* (6), 1266–1269. DOI: <https://doi.org/10.1002/aic.690190633>
- [3] T. Mattsson, M. Sedin, H. Theliander, *Sep. Purif. Technol.* **2012**, *96*, 139–146. DOI: <https://doi.org/10.1016/j.seppur.2012.05.029>
- [4] S. J. Skinner, L. J. Studer, D. R. Dixon, P. Hillis, C. A. Rees, R. C. Wall, R. G. Cavalida, S. P. Usher, A. D. Stickland, P. J. Scales, *Water Res.* **2015**, *82*, 2–13. DOI: <https://doi.org/10.1016/j.watres.2015.04.045>
- [5] K.-J. Hwang, P.-Y. Su, E. Iritani, N. Katagiri, *Sep. Sci. Technol.* **2016**, *51* (11), 1947–1953. DOI: <https://doi.org/10.1080/01496395.2016.1187629>
- [6] D. Y. Kong, S. Gerontas, R. A. McCluckie, M. Mewies, D. Gruber, N. J. Titchener-Hooker, *J. Chem. Technol. Biotechnol.* **2018**, *93* (7), 1959–1965. DOI: <https://doi.org/10.1002/jctb.5411>
- [7] E. Höfgen, S. Kühne, U. A. Peuker, A. D. Stickland, *Powder Technol.* **2019**, *346*, 49–56. DOI: <https://doi.org/10.1016/j.powtec.2019.01.056>
- [8] F. M. Tiller, C. S. Yeh, W. F. Leu, *Sep. Sci. Technol.* **1987**, *22* (2–3), 1037–1063. DOI: <https://doi.org/10.1080/01496398708068998>
- [9] R. Buscall, L. R. White, *J. Chem. Soc., Faraday Trans. 1* **1987**, *83* (3), 873. DOI: <https://doi.org/10.1039/F19878300873>
- [10] C. M. Alles, *Prozeßstrategien für die Filtration mit kompressiblen Kuchen*, Ph.D. Thesis, Universität Karlsruhe (TH) **2000**.
- [11] R. J. Wakeman, P. Wu, *KONA* **2002**, *20*, 115–124. DOI: <https://doi.org/10.14356/kona.2002014>

- [12] O. Shevchenko, S. Tynyna, *Chem. Ing. Tech.* **2017**, *89* (6), 823–830. DOI: <https://doi.org/10.1002/cite.201600019>
- [13] C. Eichholz, M. Stolarski, V. Goertz, H. Nirschl, *Chem. Eng. Sci.* **2008**, *63* (12), 3193–3200. DOI: <https://doi.org/10.1016/j.ces.2008.03.034>
- [14] E. Höfgen, D. Collini, R. J. Batterham, P. J. Scales, A. D. Stickland, *Chem. Eng. Sci.* **2019**, *205*, 106–120. DOI: <https://doi.org/10.1016/j.ces.2019.03.080>
- [15] W. Yu, N. J. D. Graham, G. D. Fowler, *Water Res.* **2016**, *95*, 1–10. DOI: <https://doi.org/10.1016/j.watres.2016.02.063>
- [16] Z.-X. Low, J. Ji, D. Blumenstock, Y.-M. Chew, D. Wolverson, D. Mattia, *J. Membr. Sci.* **2018**, *563*, 949–956. DOI: <https://doi.org/10.1016/j.memsci.2018.07.003>
- [17] A. Al-Shimmery, S. Mazinani, J. Ji, Y. J. Chew, D. Mattia, *J. Membr. Sci.* **2019**, *574*, 76–85. DOI: <https://doi.org/10.1016/j.memsci.2018.12.058>
- [18] M. T. Hung, J. C. Liu, *Sep. Purif. Technol.* **2018**, *198*, 10–15. DOI: <https://doi.org/10.1016/j.seppur.2016.10.063>
- [19] C. Fee, S. Nawada, S. Dimartino, *J. Chromatogr. A* **2014**, *1333*, 18–24. DOI: <https://doi.org/10.1016/j.chroma.2014.01.043>
- [20] P. M. Bandelt Riess, J. Engstle, M. Kuhn, H. Briesen, P. Först, *Chem. Eng. Technol.* **2018**, *41* (10), 1956–1964. DOI: <https://doi.org/10.1002/ceat.201800254>
- [21] T. Lan, S. Gerontas, G. R. Smith, J. Langdon, J. M. Ward, N. J. Titchener-Hooker, *Biotechnol. Prog.* **2012**, *28* (5), 1285–1291. DOI: <https://doi.org/10.1002/btpr.1597>
- [22] T. Lan, *An Experimental and Simulation Study of the Influence Made by Inserts on Chromatographic Packed Bed Hydrodynamics*, Ph.D. Thesis, University College London **2013**.
- [23] VDI 2762 Part 2, *Mechanical Solid-Liquid Separation by Cake Filtration. Determination of Filter Cake Resistance*, VDI guideline, Verein Deutscher Ingenieure, Düsseldorf **2010**.
- [24] M. Kuhn, P. Pergam, H. Briesen, *Chem. Eng. Technol.* **2020**, *43* (3), 493–501. DOI: <https://doi.org/10.1002/ceat.201900511>
- [25] P. Kovalsky, M. Gedrat, G. Bushell, T. D. Waite, *AIChE J.* **2007**, *53* (6), 1483–1495. DOI: <https://doi.org/10.1002/aic.11193>
- [26] W. Chen, *Drying Technol.* **2006**, *24* (10), 1251–1256. DOI: <https://doi.org/10.1080/07373930600840401>
- [27] S. P. Usher, R. G. de Kretser, P. J. Scales, *AIChE J.* **2001**, *47* (7), 1561–1570. DOI: <https://doi.org/10.1002/aic.690470709>